



Published in final edited form as:

*Small.* 2011 July 18; 7(14): 1919–1931. doi:10.1002/sml.201100442.

## More Effective Nanomedicines through Particle Design

**Dr. Jin Wang,**

Department of Chemistry, Carolina Center of Cancer Nanotechnology Excellence, Lineberger Comprehensive Cancer Center, University of North Carolina, Chapel Hill, NC 27599

**James D. Byrne,**

Department of Chemistry, Carolina Center of Cancer Nanotechnology Excellence, Lineberger Comprehensive Cancer Center, University of North Carolina, Chapel Hill, NC 27599

**Dr. Mary E. Napier,** and

Department of Chemistry, Carolina Center of Cancer Nanotechnology Excellence, Lineberger Comprehensive Cancer Center, University of North Carolina, Chapel Hill, NC 27599

**Prof. Joseph M. DeSimone\***

Departments of Chemistry and Pharmacology, Carolina Center of Cancer Nanotechnology Excellence, Institute for Advanced Materials, Institute for Nanomedicine, Lineberger Comprehensive Cancer Center, University of North Carolina, Chapel Hill, NC 27599; Department of Chemical and Biomolecular Engineering, North Carolina State University, Raleigh, NC 27695, and Sloan-Kettering Institute for Cancer Research, Memorial, Sloan-Kettering Cancer Center, New York, NY 10021

### Abstract

Nanomedicine is an emerging field that applies concepts in nanotechnology to the development of novel diagnostics and therapeutics. Physical and chemical properties of particles, including size, shape, modulus, surface charge and surface chemistry, play important roles in the efficacy of nanomedicines. This review focuses on the effect of particle physical and chemical properties on their interactions with cells *in vitro* and their pharmacokinetics and biodistribution *in vivo*.

### Keywords

Nanomedicine; Drug Delivery; PRINT

## 1. Introduction

Targeted drug delivery is one of the greatest challenges in medicine. Great strides have been made in the design and implementation of drugs and drug carriers over the last 50 years.<sup>[1–4]</sup> Nanomedicine, an emerging field that applies concepts in nanotechnology to the development of novel diagnostics and therapeutics, is shifting the paradigm in drug delivery of small molecule drugs and biologics.<sup>[1, 5, 6]</sup> Compared to small molecule therapeutics, nanomedicines can enhance drug accumulation in the site of interest while averting many of the side effects common to small molecule drugs. For example, small molecule anticancer drugs are systemically distributed and preferentially kill rapidly proliferating cells (*i.e.* cancer cells). There are significant side effects of these drugs, such as immunosuppression, hair loss, nausea, and vomiting.<sup>[7–9]</sup> Nanoparticles can encapsulate or confine small

\*Corresponding-Author: desimone@unc.edu.

(Dedicated to Dr. Mirkin)

molecule anti-cancer drug to avoid interaction with healthy cells and preferentially accumulate in the tumor through the Enhanced Permeability and Retention (EPR) effect (c.f. section 4.1).<sup>[5, 10]</sup> Furthermore, nanocarriers also play a vital role in the development of macromolecular therapeutics, such as nucleic acids (e.g. siRNA, antisense RNA) and proteins, that are difficult to deliver intracellularly.<sup>[11]</sup> Nanocarriers are also capable of removing disease-related harmful materials like molecular sponges, such as low density lipoproteins (LDLs) and cholesterol.<sup>[12, 13]</sup>

Researchers use a wide range of fabrication techniques in order to produce nanomedicines. The two major nanofabrication techniques are bottom-up fabrication techniques and top-down fabrication techniques. Bottom-up fabrication techniques involve self-assembly of molecules and atoms to create particles, and top-down fabrication techniques generate particles through the processing of bulk materials.<sup>[14]</sup> The self-assembly of amphiphilic molecules forming liposomes, micelles, and polymersomes are examples of bottom-up fabrication techniques.<sup>[15, 16]</sup> The self-assembled nature of these particles produces spherical shapes and a large size distribution. Milling and grinding of bulk materials are examples of top-down fabrication techniques. In order to produce shape-specific particles on the micron and nanometer scales, a number of advanced top-down particle fabrication techniques have been developed, such as hard template methods, microfluidics based methods, particle stretching methods and photo- and e-beam lithography.<sup>[17]</sup> Recently, our group developed a top-down fabrication technique termed Particle Replication In Non-wetting Templates (PRINT<sup>®</sup>) technology, which enables independent control over particle size, shape, modulus, surface chemistry, and composition (Figure 1). PRINT also provides a convenient approach for systematically tailoring the chemical composition of nanoparticles without changing the size, shape, and dynamics of the particle, a problem that often plagues many other particle fabrication technologies, especially those derived from self-assembly approaches when one adjusts the chemical composition.<sup>[17–28]</sup> A wide range of materials can be used for PRINT particle fabrication, including biocompatible/biodegradable polymers, inorganic materials, and biologics.

There are a number of excellent comprehensive reviews summarizing the many exciting advancements in the nanomedicine field.<sup>[1, 19, 29–44]</sup> This review will focus on the effect of particle physical and chemical properties on their interactions with cells *in vitro* and their pharmacokinetics and dynamics *in vivo*. We will cover both nanoparticles and microparticles, as microparticles also provide good insight into the development and application of drug carriers.<sup>[45–50]</sup>

## 2. Cellular Entry Pathways for Particles

Particles and macromolecules can be taken up into cells through a process called *endocytosis*.<sup>[51]</sup> There are two major mechanisms of endocytosis (Figure 2), which are *phagocytosis* (cell eating, the uptake process of large particles) and *pinocytosis* (cell drinking, the uptake process for small particles, fluid and solutes). Phagocytosis primarily occurs in macrophages and polymorphonuclear neutrophils (PMNs). In contrast, pinocytosis occurs in all types of cells through at least four distinct mechanisms: macropinocytosis, clathrin-mediated endocytosis (CME), caveolae-mediated endocytosis, and clathrin- and caveolae independent endocytosis. All of these cellular entry processes are highly regulated in order to precisely control cellular responses to the environment.<sup>[51]</sup>

### 2.1. Phagocytosis

Macrophages and PMNs are professional “eaters” that are capable of clearing foreign materials, pathogens, including bacteria or yeasts, and cellular debris. A specific signaling cascade triggers the assembly of actin, a globular 42-kDa protein, and the formation of cell-

surface protrusions that engulf the foreign material or cellular debris.<sup>[52, 53]</sup> Macrophages can engulf particles as large as 10  $\mu\text{m}$  in diameter and are one of the major barriers that limit the effective delivery of particles to the site of disease. In this review, we will mainly focus on the detailed mechanisms of pinocytosis, which are more relevant to the cellular internalization of nanomedicines.

## 2.2. Pinocytosis

Pinocytosis, or fluid-phase uptake, is the most common form of endocytosis and occurs in all cell types.<sup>[51]</sup> Solutes can nonspecifically adsorb to the cell membrane to achieve internalization (adsorptive pinocytosis). When solutes are captured by specific high-affinity receptors, they can be internalized through a receptor mediated endocytosis (RME), which is the most efficient pinocytic pathway. Overall, the pinocytotic pathway is determined by the surface interaction of the particle and the cell.

**2.2.1. Clathrin-mediated endocytosis (CME)**—Clathrin-mediated endocytosis requires the formation of coated pits by the assembly of clathrin, a protein that forms a triskelion shape composed of three clathrin heavy chains and three light chains. Coated pits develop into vesicles upon endocytosis. Two major examples of CME are the internalization of cholesterol-rich low-density lipoprotein (LDL) particles through the LDL receptor and the internalization of iron-loaded transferrin (Tf) through transferrin receptors (TfR). It is worth noting that even though both LDL and Tf are internalized through CME, their intracellular destinies are distinct; LDL is delivered to lysosomes for degradation, and Tf is recycled back to the cell surface through a recycling mechanism. The final destination of an endocytic vesicle is not only determined by the internalization mechanism but also by receptor signaling. As such, the intracellular trafficking of nanoparticles conjugated with targeting ligands will not always be the same as the trafficking pathway for the free ligand.<sup>[26, 54, 55]</sup> Detailed examples will be discussed in the next section. Vesicles formed by CME have an average size of 120 nm and are typically directed towards the lysosome for degradation of their cargo.<sup>[51]</sup> Thus, for particles internalized by CME, endosomal escape is necessary for successful delivery of macromolecules.

**2.2.2. Caveolae-mediated endocytosis**—Caveolae are small flask-shaped (50–60 nm) invaginations of the plasma membrane on many cell types, particularly endothelial cells.<sup>[51]</sup> The structure of caveolae is created by caveolin, a dimeric protein that binds cholesterol and sphingolipids in certain areas of the cell membrane and leads to the formation of caveolae. Simian virus 40 (SV40) particles are a good example of particles endocytosed through caveolae-mediated endocytosis.<sup>[56]</sup> SV40 triggers its own uptake by multivalent crosslinking of caveolae-localized surface receptors. Unlike the clathrin-mediated endocytosis, SV40 bypasses the endo-lysosomal compartments and is transported to the endoplasmic reticulum and the nucleus. This caveolae-mediated pathway can be used for targeted macromolecule delivery. The folic acid ligand has been proposed to be internalized through a caveolae-mediated pathway.<sup>[34, 57–60]</sup> Albumin is internalized by interacting with endothelium gp60 receptors through a caveolae-mediated mechanism.<sup>[35]</sup> In general, caveolae-mediated endocytosis is relatively slow (half-time,  $t_{1/2} > 20\text{min}$ ) and the vesicles formed are small (50–60 nm in diameter).<sup>[51]</sup>

**2.2.3. Clathrin- and caveolin-independent endocytosis**—Cellular entry can also occur in cells without clathrin and caveolin. There are cholesterol-rich microdomains on the plasma membrane referred to as lipid rafts (40 – 50 nm in length). For example, the interleukin-2 (IL-2) receptor on lymphocytes is internalized in a clathrin- and caveolin-independent manner.<sup>[61]</sup> These clathrin- and caveolin-independent pathways remain poorly understood.

**2.2.4. Macropinocytosis**—Macropinocytosis is a special clathrin- and caveolin-independent endocytosis. Macropinocytosis is similar to phagocytosis as it is an actin-driven process, but it is different from phagocytosis as the protrusions in macropinocytosis collapse onto and fuse with the plasma membrane to generate large endocytic vesicles (0.5–10  $\mu\text{m}$ ). Generally, macropinocytosis serve as a non-specific pathway to internalize large particles.<sup>[30]</sup>

### 3. The impact of particle design on cellular internalization

The physical and chemical properties of particles play an important role in determining the interactions with cells. We discuss how the particle size, shape, modulus, surface charge, and surface chemistry determine the cellular entry mechanisms and intracellular trafficking patterns.

#### 3.1. Particle size

Particle size is a key factor in the process of particle internalization. A generally accepted diameter of nanoparticles used to treat cancer is in the range of 10 – 100 nm, which is determined by the *in vivo* clearance and distribution of nanoparticles (*vide infra*). Even though small particles may facilitate the cellular entry process, there seems to be no size limit up to 5  $\mu\text{m}$  to gain cellular internalization.<sup>[21]</sup> Rejman et al. performed a systematic study using different sizes (50 – 1000 nm) of polystyrene beads on a murine melanoma cell line B16-F10.<sup>[62]</sup> It was reported that internalization of nanoparticles smaller than 200 nm mainly involved in clathrin-mediated endocytosis. The authors also claimed that nanoparticles with a diameter of 500 nm were internalized through the caveolae-mediated pathway bypassing lysosomal accumulation. This caveolae-mediated endocytosis of the particles contradicts the conventional notion that caveolae-mediated endocytosis is associated with the internalization of small nanoparticles (~50 – 60 nm). The Hanes group discovered that small polystyrene particles (< 25 nm) but not large particles (> 42 nm) can enter HeLa cells via a cholesterol-independent, non-clathrin and non-caveolae mediated pathway that avoids the endo/lysosomal accumulation.<sup>[63]</sup> Levy et al. reported that the cellular internalization of 100 nm PLGA particles on a gastrointestinal epithelium cell line (caco-2) is much faster than their 500 nm – 10  $\mu\text{m}$  counterparts.<sup>[64]</sup> Chan et al. investigated the interactions between a series of Herceptin<sup>®</sup> coated gold nanoparticles with well defined sizes (2 – 100 nm) and a breast cancer cell line (SK-BR-3) and demonstrated that gold nanoparticles with diameter of 40 and 50 nm can enter cells most effectively and improve the therapeutic efficacy of Herceptin.<sup>[65, 66]</sup>

Taking advantage of the PRINT technology's ability for precise control over particle size and shape, our group studied the internalization of a series of polyethylene glycol hydrogels (100 nm – 5  $\mu\text{m}$ ) on HeLa cells (Figure 3A).<sup>[21]</sup> A general trend found was that large microparticles had slower internalization kinetics compared to small nanoparticles. The internalization of these particles is through a combination of clathrin- and caveolae-mediated pathways as well as non-clathrin- and non-caveolae-mediated pathways. In summary, the rate and mechanism of cellular internalization of particles is size-dependent. For non-phagocytic cells, nanoparticles tend to achieve faster cellular entry compared to microparticles. Very small nanoparticles in the low tens of nanometer range may utilize a non-clathrin- and non-caveolae-mediated pathway avoiding endo/lysosomal degradation, which has significant implications for delivery of macromolecules.

#### 3.2. Particle Shape

As the majority of particles used for drug delivery are fabricated using the bottom-up fabrication strategy and tend to be spherical, there are a limited number studies evaluating

the relationship between particle shape and cellular internalization. The Mitragotri group fabricated a series of polystyrene particles with distinct size and shape by stretching methods and discovered that particle shape, not size, plays a key role in macrophage phagocytosis.<sup>[67–69]</sup> The tangent angles of the particle surface at the point making initial contact with macrophages need to be smaller than  $45^\circ$  to allow for particle internalization.<sup>[67]</sup> If the contact angle is larger than  $45^\circ$ , the cell can spread on the particle surface but cannot internalize it. Taking advantage of these results, the same group developed a shape-switching PLGA particle to control the particle phagocytosis by macrophages.<sup>[70]</sup> Ferrari et al. predicted that prolate ellipsoids are the most effectively attached to macrophages but are the least effectively internalized.<sup>[71]</sup> The groups of Mitragotri and Smith used prolate ellipsoids, oblate ellipsoids and spheres to study their particle shape interactions with macrophages and demonstrated Ferrari's prediction experimentally.<sup>[72]</sup>

Some very interesting observations have been made using PRINT particles by studying the internalization of a series of polyethylene glycol based hydrogels (100 nm – 5  $\mu\text{m}$ ) on HeLa cells (Figure 3A).<sup>[21]</sup> The internalization of the rod-like, high-aspect-ratio (AR) nanoparticles ( $d = 150 \text{ nm}$ ,  $h = 450 \text{ nm}$ , volume =  $0.00795 \mu\text{m}^3$ ) occurs much more rapidly and effectively than the cylindrical counterparts ( $d = 200 \text{ nm}$ ,  $h = 200 \text{ nm}$ , volume =  $0.00628 \mu\text{m}^3$ ), even though they have very similar volume, indicating the particle shape plays a great role in the internalization process. To further elucidate the cellular internalization mechanisms, the endocytosis of three types of particles, 150 nm (AR = 3), 200 nm (AR = 1), and 1  $\mu\text{m}$  (AR = 1), was investigated using different biochemical inhibitors of energy-dependent processes, clathrin-mediated endocytosis, caveolae-mediated endocytosis, and macropinocytosis (Figure 3B). These particles were internalized through an energy-dependent pathway based on a  $\text{NaN}_3$  inhibition experiment. In the presence of three inhibitors for clathrin-mediated endocytosis, Dynasore, genistein, and chlorpromazine, both 150 nm and 200 nm particles showed markedly decrease in cell uptake; the internalization of the 1  $\mu\text{m}$  particles was only significantly affected by chlorpromazine. It is clear that the nanoparticles, at least in part, enter cells through clathrin-mediated pathway. But the cell entry mechanism cannot be delineated for 1  $\mu\text{m}$  particles. In the presence of two inhibitors for caveolae-mediated endocytosis, genistein, and  $\beta$ -cyclodextrin, the internalization was retarded for the small nanoparticles but not the large microparticles. Since caveolae have a cavity of  $\sim 60 \text{ nm}$ , microparticle internalization through a caveolae-mediated pathway was not expected. In addition, inhibition of  $>95\%$  particle internalization was not found for any inhibitor, indicating the possibility for nonclathrin- and non-caveolae-mediated pathways for internalization.

The Chan group reported that rod-like gold nanoparticles ( $14 \times 40 \text{ nm}$  and  $14 \times 74 \text{ nm}$ ) entered cells less effectively compared to their spherical counterparts (74 nm in diameter).<sup>[65]</sup> But it is worth noting that the surface of the gold nanorods was stabilized with cetyl trimethylammonium bromide (CTAB), which is different from the citric acid-coated spherical gold nanoparticles. The difference in surface chemistry may explain the disparity in particle internalization.<sup>[65]</sup> In a follow-up study by the same group, transferrin-coated gold nanorods was also internalized slower than transferrin-coated spherical gold nanoparticles.<sup>[73]</sup> The studies by the DeSimone and Chan groups present contradictory results. The studies of the impact of particle shape and cell interactions are still in their infancy and more systems need to be explored.

### 3.3. Particle Modulus

The modulus of particles is another important parameter to induce or prevent particle internalization.<sup>[40]</sup> Macrophages are trained to clear bacteria and other pathogens, which usually have very rigid cell walls. Beningo and Wang reported that soft polyacrylamide



beads (1 – 6  $\mu\text{m}$ ) frustrate the actin filament formation by macrophages and subsequently prevent phagocytosis, whereas their stiff counterparts can be readily internalized.<sup>[74]</sup> However, Lee et al. showed that rigid liposomes can decrease complement activation and reduce subsequent macrophage uptake.<sup>[75]</sup> In a recent study by Merkel et al., very soft red blood cell mimics can circulate several days, a 30-fold increase of elimination half-life compared to their rigid counterparts.<sup>[28]</sup> But both the soft and rigid particles showed very minimal uptake on human umbilical vein endothelial cells (HUVEC), probably due to their large sizes. No conclusive relationship has emerged between the particle modulus and cellular internalization process.

### 3.4. Particle Surface Charge

In general, nanoparticles with positively charged surfaces can be effectively internalized by cells through electro-static interactions with the negatively charged cell plasma membrane (adsorptive endocytosis, possibly involving CME). There are numerous examples of positively charged particles for cellular internalization, such as PLL modified PLGA, chitosan, searylamine-coated PEG-co-PLA etc.<sup>[38, 76, 77]</sup> The DeSimone group has also reported that by keeping the size and shape of particles constant, positively charged nanoparticles were internalized in 84% of cells after 1-hr incubation, whereas the negatively charged counterparts were not internalized (< 5%).<sup>[21]</sup>

On the other hand, negatively charged nanoparticles, such as DOXIL<sup>®</sup> and micelles are more likely to take advantage of caveolae-mediated pathways.<sup>[78]</sup> It also has been reported that negatively charged PLGA nanoparticles (~100 nm) can enter cells through caveolae-independent pathways.<sup>[79–81]</sup> The Mirkin group successfully demonstrated the use of 13 nm gold nanoparticles for gene delivery.<sup>[82–84]</sup> The gold nanoparticles were negatively charged, but they were effectively internalized and delivered the nucleic acids to the cytosol and nucleus.

### 3.5. Particle Surface Chemistry

Surface modification of particles is an area of intense investigation for tissue and cell-specific delivery. A number of targeting strategies and surface chemistry have been developed.<sup>[41]</sup> A general targeting strategy takes advantage of the over-expression of certain cell surface receptors. Nanoparticles conjugated with molecules that can specifically bind to the receptors are expected to boost the particle avidity (i.e. multivalent affinity) to cells. Transferrin receptors are overexpressed on the majority of cancer cells and are widely used as a cancer cell target.<sup>[85]</sup> Transferrin and transferrin receptor antibodies have also been used for site-specific drug delivery for various systems, including protein/toxin conjugates, polymer/drug conjugates, modified viral vectors, liposomes/polyplexes, and nanoparticles.<sup>[5, 86, 87]</sup> Two types of liposomal formulations for targeted drug/gene delivery, MBP-426 and SGT-53 that are currently under phase I clinical trials, utilize transferrin and an anti-transferrin receptor single-chain antibody fragment as targeting moieties, respectively.<sup>[5]</sup> The Davis group developed the most successful targeted delivery system to date for small interfering RNA (siRNA), transferrin-conjugated cyclodextrin polymer-based NPs (CALAA-01), that is undergoing a phase I clinical trial.<sup>[11, 88–93]</sup> FDA approved monoclonal antibodies have also been used as targeting ligands, such as Herceptin<sup>®</sup> and Rituxan<sup>®</sup>.<sup>[66, 94, 95]</sup> The Schnitzer group reported that aminopeptidase P antibody conjugated gold nanoparticles can be transported into endothelium cells through a caveolae mediate mechanism.<sup>[35, 96–99]</sup> Small peptides have also been explored as targeting ligands, such as the RGD peptide.<sup>[100, 101]</sup> Aptamers, single-strand short nucleic acids, are a class of new targeting ligands, which can bind any target, including proteins and small molecules, with very high affinity.<sup>[102–104]</sup> The Langer and Farokhzad groups developed nanoparticle-aptamer bioconjugates for cancer targeting.<sup>[105–110]</sup> Small molecule ligands can also be used

as targeting moieties. Pioneered by the Low group, folic acid has been widely used as a targeting ligand for drug conjugates, liposomes and nanoparticles.<sup>[34]</sup> Sigma receptors ( $\sigma_1$ ,  $\sigma_2$ ) have been targeted by Huang and colleagues using anisamide as a high-affinity sigma-receptor ligand.<sup>[111–118]</sup> Liposomes conjugated with anisamide can substantially improve the delivery of chemotherapeutics and siRNA to tumors. Mukherjee et al. reported that haloperidol, another sigma-receptor ligand, can increase DNA delivery efficiency by 10-fold to breast carcinoma cells.<sup>[119]</sup>

Not only boosting avidity to cells, multivalent ligands on nanoparticles can also have an impact on cell biology that cannot be achieved by the monovalent form of ligands.<sup>[26, 66, 120–122]</sup> Our group recently discovered that multivalent presentation of transferrin, the fourth most abundant serum protein in humans, on nanoparticles can transform this benign protein into a potential “drug-free” chemotherapy against a B-cell lymphoma.<sup>[26]</sup> Kopecek *et al.* also took advantage of the multivalent ligands to crosslink CD20 receptors to induce apoptosis in B cells.<sup>[123]</sup> Multivalent presentation of certain monoclonal antibodies on nanoparticles has been reported to enhance the therapeutic efficacy of the antibody.<sup>[66, 95]</sup> Tan *et al.* fabricated dinitrophenyl conjugated gold nanoparticles with well-controlled ligand density and showed that these multivalent nanoparticles can regulate signaling in mast cells as a function of particle size and surface ligand density.<sup>[116]</sup> Multivalent nanoparticles can also inhibit HIV fusion to human T cells and kill multidrug resistant bacteria, where the monovalent ligands did not show any biological activity.<sup>[121, 122]</sup>

It is worth noting that the cellular trafficking mechanisms for multivalent ligand conjugated nanoparticles may be different from the monovalent ligand. Endothelial cells express intercellular adhesion molecule 1 (ICAM-1) but do not internalize ICAM-1 antibodies. However, anti-ICAM-1 antibody-coated nanoparticles can be readily taken up by endothelial cells through a unique cell adhesion molecule (CAM)-mediated endocytosis, which is different from clathrin-, caveolae-, macropinocytosis- and phagocytosis-mediated pathways.<sup>[124]</sup> Mukherjee *et al.* also demonstrated that upon multivalent presentation on nanoparticles, the patterning and dynamics of anti-EGFR (epidermal growth factor receptor) antibody cetuximab is distinct from its monovalent form.<sup>[125]</sup> Iversen *et al.* showed that transferrin conjugated quantum dots were internalized through clathrin-mediated endocytosis, but the exocytosis pathway of free transferrin was blocked.<sup>[55]</sup>

#### 4. The impact of particle design on biodistribution and pharmacokinetics

The size, shape, modulus, and surface chemistry of particles also play an important role in the biodistribution and pharmacokinetics. Fundamental *in vivo* studies regarding particle design enable the engineering of better medicines for the treatment of a variety of diseases. There remains much to be elucidated, but the impact of particle design has proven to be important for drug delivery.

##### 4.1. Particle Size

Particle size is an important component in the design of long-circulating particle systems. As discussed previously, the generally accepted diameter of nanomedicine for cancer is in the range of 10 – 100 nm. The lower limit is determined by the sieving coefficients for the glomerular capillary wall in the kidney to avoid renal filtration.<sup>[126]</sup> Particles of sizes ranging from 10 nm to 15  $\mu\text{m}$  have different pharmacokinetic parameters and biodistribution. Under normal homeostatic conditions, large particles are mechanically filtered through the spleen and liver by the reticuloendothelial system (RES). The RES, one of the body's defense and filtration mechanisms, functions to remove old or irregular red and white blood cells, as well as opsonized constituents and large foreign objects.

Fenestrations in the spleen are typically 200 – 500 nm in width, and thus, particles larger than 200 nm must compensate by deformability.<sup>[42]</sup> For certain diseases, such as cancer, size of particles can play a large role in accumulation of the particles for therapeutic and diagnostic purposes. Solid tumors typically present with aberrant angiogenic vasculature that enables passive accumulation of particles. In a human colon adenocarcinoma xenograft model, the cutoff size of the vascular pores was determined to be 400 – 600 nm in diameter.<sup>[127]</sup> Characteristic solid tumors have higher interstitial pressure in the center of the tumor compared to the periphery. An outward convective flow reduces drug diffusion to the center of the tumor, and particles and drugs that gain interstitial access have higher retention times than in normal tissues. This aberrant vasculature and higher interstitial fluid pressure create an enhanced permeability and retention of the nanoparticles. Particles that are smaller than the fenestration can gain access and be retained in the tumor.<sup>[41, 42, 128]</sup>

#### 4.2. Particle Shape

The importance of particle shape has derived the morphological adaptation of pathogens in nature. The shape of the pathogen serves a critical biological function, where infectious and metastatic agents with different shapes, sizes, and moduli can cope with and adapt to external conditions. Examples in nature are influenza, ebola, and filoviruses — these are viruses with morphologies that have been subject to the selective forces of survival and proliferation.<sup>[129]</sup> Exploiting the self-assembly characteristics of symmetric amphiphiles, Geng *et al.* created worm-like particles, termed filomicelles, and evaluated their circulation times *in vivo* and anti-cancer efficacy (Figure 4).<sup>[130]</sup> The filomicelles were created from one of two materials, PEG:polyethylene (inert) and PEG:polycaprolactone (biodegradable). The pharmacokinetics of the filomicelles was evaluated using fluorescence imaging of a hydrophobic dye that was retained within the particles. The particles were shown to circulate for up to one week in rodents, and the circulation time of the filomicelles show a dependence upon length of the particle. PEGylated ‘stealth’ vesicles were also evaluated and found to be cleared within two days. Particles of an initial length of 8  $\mu\text{m}$  persist longest in circulation; however, particles longer than 8  $\mu\text{m}$  underwent rapid chain scission.

Paclitaxel-loaded filomicelles were evaluated as a cancer therapy.<sup>[130]</sup> Tumor-bearing nude mice (A549 subcutaneous xenograft tumors) were administered 1  $\mu\text{m}$  or 8  $\mu\text{m}$  particles via intravenous injection. The results seven days post-injection showed that filomicelles provided an advantage as a drug carrier compared to the controls of free drug. An eight-fold increase in the length of the filomicelle was equivalent to an eight-fold increase in drug administration. The 1  $\mu\text{m}$  or 8  $\mu\text{m}$  particles provided similar reductions in tumor burden and a doubling of the apoptosis after one week.

Furthermore, the circulation times and endothelial cell targeting of intravenously injected ICAM-1-targeted elliptical disks ( $0.1 \times 1 \times 3 \mu\text{m}$ ) and ICAM-1-targeted spheres (0.1, 1, 5, and 10  $\mu\text{m}$ ) were evaluated in C57Bl/6 mice.<sup>[54]</sup> The 0.1  $\mu\text{m}$  ICAM-1-targeted spheres were rapidly cleared from the blood post-injected, with  $16.2 \pm 2.7\%$  of the injected dose (%ID) and  $5.2 \pm 0.5\%$  ID remaining in the blood 1 minute and 30 minutes post-injection, respectively. Hepatic uptake of these carriers was substantial at  $43.7 \pm 4.5\%$  of the ID per gram of organ tissue. Pulmonary uptake was significant compared to the non-targeted control spheres, showing  $114.7 \pm 11.1\%$  ID/g versus  $10.2 \pm 3.9\%$  ID/g, respectively. The larger ICAM-1-targeted spheres were cleared faster than the 0.1  $\mu\text{m}$  ICAM-1-targeted spheres. The ICAM-1-targeted elliptical disks remained in circulation longer than the spheres, with  $25.5 \pm 2.8\%$  ID and  $20.9 \pm 1.6\%$  ID remained in the blood at 1 and 30 minutes post-injection, respectively. There was much lower hepatic uptake ( $15.7 \pm 2.3\%$  ID/g) and significant pulmonary uptake ( $186.2 \pm 15.4\%$  ID/g). Thus, the elliptical disks showed greater pulmonary targeting compared to spherical particles.<sup>[54]</sup>



### 4.3. Particle Modulus

A difference between the moduli of metastatic cancer cells and non-metastatic cancer cells has been discovered, and this difference in modulus has been thought to be a major mechanism enabling these cells to relocate and take hold in other parts of the body.<sup>[131, 132]</sup>

Modulus was evaluated using red blood cell mimic (RBCM) hydroxyethyl acrylate (HEA) hydrogel PRINT<sup>®</sup> particles.<sup>[28]</sup> The RBCMs were negatively charged, micron-sized, biconcave disks that were the same size as mouse red blood cells (6  $\mu\text{m}$ ) and were used to evaluate the influence of modulus on circulation times (Figure 5A). Tensile testing of macroscopic coupons of these hydrogels was performed at varying percentages of the crosslinker, poly(ethylene glycol diacrylate) (PEGDA) (neutral pH), resulting in a modulus ranging from  $63.9 \pm 15.7$  to  $7.8 \pm 10.0$  kPa (Figure 5B). A reduction in the cross-linking density exhibited modulus values within the range of red blood cells ( $26 \pm 7$  kPa). Scaled-down master templates were fabricated to allow the RBCMs to swell to the desired dimensions upon hydration, yielding discs that were 5.2–5.9  $\mu\text{m}$  in diameter and 1.22–1.54  $\mu\text{m}$  tall, with the feature size and final RBCM dimensions dependent upon the percent of cross-linker. The filling of the molds resulted in a meniscal effect, yielding RBCMs that were similar to the biconcave shape of red blood cells (Figure 5A). A near IR dye (Dylight<sub>680</sub> maleimide) was used for *in vivo* imaging in mice.

The RBCMs were initially evaluated using microfluidic models of vascular constriction. The more deformable (1 and 2% crosslinked) RBCMs were found to be able to navigate 3  $\mu\text{m}$  wide and 50  $\mu\text{m}$  long channels (Figure 5D), while the more rigid (5 and 10% crosslinked) RBCMs clogged the channels (Figure 5C). The more deformable RBCMs retained their shape after distorting many times, reverting back to their original shape once flow was halted. Intravital microscopy was used to evaluate the microcirculation of the intravenously injected RBCMs. For *in vivo* studies, the peripheral vasculature of an anesthetized mouse's ear was observed, and the near-IR fluorescence of the particles was evaluated over a two-hour time course wherein elimination curves were generated. The most rigid RBCMs were cleared quite rapidly, while the most deformable RBCMs were eliminated over 30 times more slowly. The most deformable RBCMs were also monitored using the more traditional blood-draw method. The pharmacokinetic analysis of this data was consistent with the data obtained using the intravital microscope, showing an elimination half-life of 3.8 days with 5% of the injected dose remaining in the blood after 5 days.<sup>[133]</sup>

Evaluation of the biodistribution of the RBCMs after two hours post-injection revealed large lung accumulation for the most rigid particles (Figure 6), which is typical for intravenously-injected microparticles. The bulk of the dose was sequestered through the first pass. The stiffer RBCMs were poorly tolerated while the more flexible RBCMs were well tolerated due to the avoidance of filtration in the lung. The more flexible RBCMs were largely sequestered into spleen. Lung filtration was avoided by particles with 2% or less cross-linker, and kidney filtration was significant for all but 1% of the crosslinked RBCMs.<sup>[133]</sup> Thus, modulus was found to play an important role in particle pharmacokinetics and biodistribution.

### 4.4 Particle Surface Charge

Surface charge plays a significant role in nonspecific cellular internalization and protein absorption in circulation. Particles with a positively charged surface are expected to have high nonspecific internalization rate and short blood circulation half-life. It has been found that polystyrene microparticles with primary amine surface functionalities undergo substantially more phagocytosis compared to the same particles with carboxyl, sulfate, and hydroxyl groups.<sup>[134]</sup> Yamamoto *et al.* evaluated surface charge on poly(ethylene glycol)-

poly(D, L-lactide) block copolymer micelles using neutral (tyrosine) and negative (tyrosine-glutamine) functionalities. No difference was found between blood clearance kinetics, but the negatively-charged micelles displayed a 10x lower accumulation in liver and spleen four hours post-intravenous administration.<sup>[135]</sup> He *et al.* evaluated negatively charged (rhodamine B labeled carboxymethyl chitosan grafted) nanoparticles and positively charged (chitosan hydrochloride grafted nanoparticles) for cellular uptake and biodistribution.<sup>[136]</sup> Particles with a surface charge below 15 mV showed a reduction in phagocytic uptake by murine macrophages, and the particles with lower surface charges promoted longer blood residence time and higher accumulation in the tumors of subcutaneous xenograft H-22 tumor-bearing mice.

#### 4.5. Particle Surface Chemistry

The surface properties of a particle can affect its interactions with molecules, cells, or physiological systems in the body and impart a variety of desirable characteristics for the delivery of therapeutics and diagnostics. For example, the chemical conjugation of PEG groups onto the surface of particles has enabled stealth-like properties when in circulation. The PEG groups have the ability to reduce non-specific uptake by cells, to diminish adsorption by proteins and other biomolecules in the serum, and to elude phagocytosis by macrophages, all of which contribute to longer circulation time.<sup>[137]</sup> Another desirable characteristic for particles in biomedical applications is the ability to selectively interact with specific cell types such as cancer cells. This selectivity can ensure that an effective amount of the therapeutic payload will be delivered to the target cells of interest, thereby minimizing the potential side effects that accompany intravenous chemotherapy. Li and Huang have proposed that ideal particle delivery systems transport to the target site at > 10% injected dose in 4 hours and are cleared from circulation between 4 and 10 hours for safety. PEG density plays an important role, and for the treatment of cancer, it has been proposed that high density and sheddable PEG chains are the key for tumor targeting.<sup>[128]</sup>

Surface modification with targeting moieties is advantageous for cellular endocytosis after particle accumulation in the site of interest. Weissleder *et al.* used a combinatorial approach to find targeting moieties for cells of interest. This approach involved the creation of 146 iron oxide nanoparticles decorated with different synthetic small molecules.<sup>[138]</sup> The library created was tested for specificity for endothelial cells (HUVEC), activated human macrophages (U937), and pancreatic cancer cells (PaCa-2), and small molecules were delineated for their specificity to each system. Fourteen candidates showed significant uptake in the pancreatic cancer cells, and from these fourteen, two candidates exhibited high pancreatic cancer cell uptake and low macrophage/endothelial cell uptake. The two candidates were isatoic anhydride (designated 261-15-28) and 5-chloro-isatoic anhydride (261-14-17). Fluorescently labeled candidates (CLIO-isatoic-Cy5.5) were intravenously injected into subcutaneous xenograft mice and were compared with a control group CLIO-NH<sub>2</sub>-Cy3.5 using fluorescence imaging (TBR of 1.62 versus 0.16, p value < 0.0001). The results proved an increase in pancreatic cancer detection in the mouse model using the targeting moiety.<sup>[138]</sup>

## 5. Conclusions

In summary, the following physical parameters for effective nanomedicines are recommended:

- Size: Particles in the range of 10–100 nm can avoid renal filtration and are small enough to efficiently accumulate in tumors through the EPR effect. However, microparticles may be better suited for vascular targeting than nanoparticles.

- **Shape:** Certain shape specific delivery systems have demonstrated advantages over spherical systems. Filamentous particles can help evade macrophage uptake, and shape-specific microparticles can enhance vascular adhesion.
- **Modulus:** Soft particles can navigate through pores smaller than the size of particles and achieve extended circulation.
- **Surface charge and surface chemistry:** Neutral PEGylated particles are ideal to avoid macrophage uptake. Introducing targeting ligands can also potentially enhance cancer cell uptake.

Future studies in this field should focus on creating more effective nanomedicines by designing particles to target certain organs, control particle intracellular trafficking pathways and deliver cargo to intracellular organelles.

## Acknowledgments

This work was supported in part by the STC Program of the National Science Foundation (CHE-9876674), National Institutes of Health Program Project Grant PO1-GM059299, National Institutes of Health Grants U54-CA119343 (the Carolina Center of Cancer Nanotechnology Excellence) and R01-EB009565, Prostate Cancer Foundation, University of North Carolina Cancer Research Fund, the Chancellor's Eminent Professorship and William R. Kenan Professorship at the University of North Carolina at Chapel Hill, and a sponsored research agreement with Liquidia Technologies.

## References

1. Riehemann K, Schneider S, Luger T, Godin B, Ferrari M, Fuchs H. *Angew Chem Int Ed.* 2009; 48:872.
2. Singh R, Lillard J. *Experimental and Molecular Pathology.* 2009; 86:215. [PubMed: 19186176]
3. Debbage P. *Curr Pharm Des.* 2009; 15:153. [PubMed: 19149610]
4. Muthu M, Singh S. *Nanomedicine.* 2009; 4:105. [PubMed: 19093899]
5. Heath JR, Davis ME. *Annu Rev Med.* 2008; 59:251. [PubMed: 17937588]
6. Doshi N, Mitragotri S. *Advanced Functional Materials.* 2009; 19:3843.
7. Chaffer CLW, Robert A. *Science.* 2011; 331:1559. [PubMed: 21436443]
8. Marshall E. *Science.* 2011; 331:1540. [PubMed: 21436436]
9. Stratton MR. *Science.* 2011; 331:1553. [PubMed: 21436442]
10. Davis ME, Chen ZG, Shin DM. *Nat Rev Drug Discov.* 2008; 7:771. [PubMed: 18758474]
11. Davis ME. *Mol Pharm.* 2009; 6:659. [PubMed: 19267452]
12. Thaxton CS, Daniel WL, Giljohann DA, Thomas AD, Mirkin CA. *J Am Chem Soc.* 2009; 131:1384. [PubMed: 19133723]
13. Luthi AJ, Patel PC, Ko CH, Mutharasan RK, Mirkin CA, Thaxton CS. *Trends Mol Med.* 2010; 16:553. [PubMed: 21087901]
14. Nalwa, H. *Nanostructured materials and nanotechnology.* Academic Pr; 2002.
15. Discher DE, Ahmed F. *Annu Rev Biomed Eng.* 2006; 8:323. [PubMed: 16834559]
16. Immordino ML, Dosio F, Cattel L. *Int J Nanomedicine.* 2006; 1:297. [PubMed: 17717971]
17. Merkel TJ, Herlihy KP, Nunes J, Orgel RM, Rolland JP, DeSimone JM. *Langmuir.* 2010; 26:13086. [PubMed: 20000620]
18. Rolland J, Maynor B, Euliss L, Exner A, Denison G, DeSimone J. *Journal of the American Chemical Society.* 2005; 127:10096. [PubMed: 16011375]
19. Euliss L, DuPont J, Gratton S, DeSimone J. *Chemical Society Reviews.* 2006; 35:1095. [PubMed: 17057838]
20. Gratton SE, Napier ME, Ropp PA, Tian S, DeSimone JM. *Pharmaceutical Research.* 2008; 25:2845. [PubMed: 18592353]
21. Gratton SEA, Ropp PA, Pohlhaus PD, Luft JC, Madden VJ, Napier ME, DeSimone JM. *Proceedings of the National Academy of Sciences, USA.* 2008; 105:11613.

22. Kelly J, DeSimone J. *Journal of the American Chemical Society*. 2008; 130:5438. [PubMed: 18376832]
23. Zhang H, Nunes J, Gratton S, Herlihy K, Pohlhaus P, DeSimone J. *New Journal of Physics*. 2009; 11:075018.
24. Jeong W, Napier ME, DeSimone JM. *Nanomedicine (Lond)*. 2010; 5:633. [PubMed: 20528457]
25. Parrott MC, Luft JC, Byrne JD, Fain JH, Napier ME, Desimone JM. *J Am Chem Soc*. 2010; 132:17928. [PubMed: 21105720]
26. Wang J, Tian S, Petros RA, Napier ME, Desimone JM. *J Am Chem Soc*. 2010; 132:11306. [PubMed: 20698697]
27. Enlow EM, Luft JC, Napier ME, Desimone JM. *Nano Lett*. 2011; 11:808. [PubMed: 21265552]
28. Merkel TJ, Jones SW, Herlihy KP, Kersey FR, Shields AR, Napier M, Luft JC, Wu H, Zamboni WC, Wang AZ, Bear JE, DeSimone JM. *Proc Natl Acad Sci U S A*. 2011; 108:586. [PubMed: 21220299]
29. Verma A, Stellacci F. *Small*. 2010; 6:12. [PubMed: 19844908]
30. Sahay G, Alakhova DY, Kabanov AV. *J Control Release*. 2010; 145:182. [PubMed: 20226220]
31. Park S, Hamad-Schifferli K. *Curr Opin Chem Biol*. 2010; 14:616. [PubMed: 20674473]
32. Hillaireau H, Couvreur P. *Cell Mol Life Sci*. 2009; 66:2873. [PubMed: 19499185]
33. Bareford LM, Swaan PW. *Adv Drug Deliv Rev*. 2007; 59:748. [PubMed: 17659804]
34. Lu Y, Low PS. *Adv Drug Deliv Rev*. 2002; 54:675. [PubMed: 12204598]
35. Schnitzer JE. *Adv Drug Deliv Rev*. 2001; 49:265. [PubMed: 11551399]
36. Discher DE, Eisenberg A. *Science*. 2002; 297:967. [PubMed: 12169723]
37. Yoo JW, Chambers E, Mitragotri S. *Curr Pharm Des*. 2010; 16:2298. [PubMed: 20618151]
38. Harush-Frenkel O, Altschuler Y, Benita S. *Crit Rev Ther Drug Carrier Syst*. 2008; 25:485. [PubMed: 19166392]
39. Rosi N, Mirkin C. *Chemical reviews*. 2005; 105:1547. [PubMed: 15826019]
40. Kabanov AV, Vinogradov SV. *Angew Chem Int Ed Engl*. 2009; 48:5418. [PubMed: 19562807]
41. Byrne JD, Betancourt T, Brannon-Peppas L. *Advanced drug delivery reviews*. 2008; 60:1615. [PubMed: 18840489]
42. Petros RA, DeSimone JM. *Nat Rev Drug Discov*. 2010; 9:615. [PubMed: 20616808]
43. Sanhai W, Sakamoto J, Canady R, Ferrari M. *Nature Nanotechnology*. 2008; 3:242.
44. Chou LY, Ming K, Chan WC. *Chem Soc Rev*. 2011; 40:233. [PubMed: 20886124]
45. Decuzzi P, Ferrari M. *Biomaterials*. 2008; 29:377. [PubMed: 17936897]
46. Lee S-Y, Ferrari M, Decuzzi P. *Journal of Biomechanics*. 2009; 42:1885. [PubMed: 19523635]
47. Lee S-Y, Ferrari M, Decuzzi P. *Nanotechnology*. 2009; 20:495101. [PubMed: 19904027]
48. Serda RE, Gu J, Bhavane RC, Liu X, Chiappini C, Decuzzi P, Ferrari M. *Biomaterials*. 2009; 30:2440. [PubMed: 19215978]
49. Decuzzi P, Godin B, Tanaka T, Lee SY, Chiappini C, Liu X, Ferrari M. *Journal of Controlled Release*. 2010; 141:320. [PubMed: 19874859]
50. Decuzzi P, Ferrari M. *Biomaterials*. 2006; 27:5307. [PubMed: 16797691]
51. Conner SD, Schmid SL. *Nature*. 2003; 422:37. [PubMed: 12621426]
52. Aderem A, Underhill DM. *Annu Rev Immunol*. 1999; 17:593. [PubMed: 10358769]
53. Chimini G, Chavrier P. *Nat Cell Biol*. 2000; 2:E191. [PubMed: 11025683]
54. Muro S, Garnacho C, Champion JA, Leferovich J, Gajewski C, Schuchman EH, Mitragotri S, Muzykantov VR. *Mol Ther*. 2008; 16:1450. [PubMed: 18560419]
55. Tekle C, Deurs B, Sandvig K, Iversen TG. *Nano Lett*. 2008; 8:1858. [PubMed: 18570482]
56. Pelkmans L, Puntener D, Helenius A. *Science*. 2002; 296:535. [PubMed: 11964480]
57. Rothberg KG, Ying YS, Kolhouse JF, Kamen BA, Anderson RG. *J Cell Biol*. 1990; 110:637. [PubMed: 1968465]
58. Mayor S, Rothberg KG, Maxfield FR. *Science*. 1994; 264:1948. [PubMed: 7516582]
59. Wu M, Fan J, Gunning W, Ratnam M. *J Membr Biol*. 1997; 159:137. [PubMed: 9307440]

60. Varma R, Mayor S. *Nature*. 1998; 394:798. [PubMed: 9723621]
61. Lamaze C, Dujeancourt A, Baba T, Lo CG, Benmerah A, Dautry-Varsat A. *Mol Cell*. 2001; 7:661. [PubMed: 11463390]
62. Rejman J, Oberle V, Zuhorn IS, Hoekstra D. *Biochem J*. 2004; 377:159. [PubMed: 14505488]
63. Lai SK, Hida K, Man ST, Chen C, Machamer C, Schroer TA, Hanes J. *Biomaterials*. 2007; 28:2876. [PubMed: 17363053]
64. Desai MP, Labhasetwar V, Walter E, Levy RJ, Amidon GL. *Pharm Res*. 1997; 14:1568. [PubMed: 9434276]
65. Chithrani BD, Ghazani AA, Chan WC. *Nano Lett*. 2006; 6:662. [PubMed: 16608261]
66. Jiang W, Kim BY, Rutka JT, Chan WC. *Nature Nanotechnology*. 2008; 3:145.
67. Champion JA, Mitragotri S. *Proc Natl Acad Sci U S A*. 2006; 103:4930. [PubMed: 16549762]
68. Doshi N, Mitragotri S. *PLoS One*. 2010; 5:e10051. [PubMed: 20386614]
69. Champion JA, Katare YK, Mitragotri S. *Proc Natl Acad Sci U S A*. 2007; 104:11901. [PubMed: 17620615]
70. Yoo JW, Mitragotri S. *Proc Natl Acad Sci U S A*. 2010; 107:11205. [PubMed: 20547873]
71. Decuzzi P, Ferrari M. *Biophysical journal*. 2008; 94:3790. [PubMed: 18234813]
72. Sharma G, Valenta DT, Altman Y, Harvey S, Xie H, Mitragotri S, Smith JW. *J Control Release*. 2010; 147:408. [PubMed: 20691741]
73. Chithrani BD, Chan WC. *Nano Lett*. 2007; 7:1542. [PubMed: 17465586]
74. Beningo KA, Wang YL. *J Cell Sci*. 2002; 115:849. [PubMed: 11865040]
75. Allen TM, Austin GA, Chonn A, Lin L, Lee KC. *Biochim Biophys Acta*. 1991; 1061:56. [PubMed: 1995057]
76. Harush-Frenkel O, Debotton N, Benita S, Altschuler Y. *Biochem Biophys Res Commun*. 2007; 353:26. [PubMed: 17184736]
77. Harush-Frenkel O, Rozentur E, Benita S, Altschuler Y. *Biomacromolecules*. 2008; 9:435. [PubMed: 18189360]
78. Sahay G, Kim JO, Kabanov AV, Bronich TK. *Biomaterials*. 2010; 31:923. [PubMed: 19853293]
79. Panyam J, Labhasetwar V. *Pharm Res*. 2003; 20:212. [PubMed: 12636159]
80. Panyam J, Sahoo SK, Prabha S, Bargar T, Labhasetwar V. *Int J Pharm*. 2003; 262:1. [PubMed: 12927382]
81. Qaddoumi MG, Ueda H, Yang J, Davda J, Labhasetwar V, Lee VH. *Pharm Res*. 2004; 21:641. [PubMed: 15139521]
82. Rosi N, Giljohann D, Thaxton C, Lytton-Jean A, Han M, Mirkin C. *Science*. 2006; 312:1027. [PubMed: 16709779]
83. Giljohann D, Seferos D, Prigodich A, Patel P, Mirkin C. *Journal of the American Chemical Society*. 2009; 131:2072. [PubMed: 19170493]
84. Zheng D, Seferos DS, Giljohann DA, Patel PC, Mirkin CA. *Nano Lett*. 2009; 9:3258. [PubMed: 19645478]
85. Li H, Qian ZM. *Med Res Rev*. 2002; 22:225. [PubMed: 11933019]
86. Daniels TR, Delgado T, Helguera G, Penichet ML. *Clin Immunol*. 2006; 121:159. [PubMed: 16920030]
87. Daniels TR, Delgado T, Rodriguez JA, Helguera G, Penichet ML. *Clin Immunol*. 2006; 121:144. [PubMed: 16904380]
88. Bellocq NC, Pun SH, Jensen GS, Davis ME. *Bioconjugate Chem*. 2003; 14:1122.
89. Hu-Lieskovan S, Heidel JD, Bartlett DW, Davis ME, Triche TJ. *Cancer Res*. 2005; 65:8984. [PubMed: 16204072]
90. Bartlett D, Davis M. *Bioconjugate Chem*. 2007; 18:456.
91. Heidel JD, Yu Z, Liu JY, Rele SM, Liang Y, Zeidan RK, Kornbrust DJ, Davis ME. *Proc Natl Acad Sci USA*. 2007; 104:5715. [PubMed: 17379663]
92. Choi CHJ, Alabi CA, Webster P, Davis ME. *Proc Natl Acad Sci USA*. 2010; 107:1235. [PubMed: 20080552]



93. Davis ME, Zuckerman JE, Choi CH, Seligson D, Tolcher A, Alabi CA, Yen Y, Heidel JD, Ribas A. *Nature*. 2010; 464:1067. [PubMed: 20305636]
94. Ishida O, Maruyama K, Tanahashi H, Iwatsuru M, Sasaki K, Eriguchi M, Yanagie H. *Pharm Res*. 2001; 18:1042. [PubMed: 11496943]
95. Chiu GN, Edwards LA, Kapanen AI, Malinen MM, Dragowska WH, Warburton C, Chikh GG, Fang KY, Tan S, Sy J, Tucker C, Waterhouse DN, Klasa R, Bally MB. *Mol Cancer Ther*. 2007; 6:844. [PubMed: 17339368]
96. McIntosh DP, Tan XY, Oh P, Schnitzer JE. *Proc Natl Acad Sci U S A*. 2002; 99:1996. [PubMed: 11854497]
97. Oh P, Li Y, Yu J, Durr E, Krasinska KM, Carver LA, Testa JE, Schnitzer JE. *Nature*. 2004; 429:629. [PubMed: 15190345]
98. Oh P, Borgstrom P, Witkiewicz H, Li Y, Borgstrom BJ, Chrastina A, Iwata K, Zinn KR, Baldwin R, Testa JE, Schnitzer JE. *Nat Biotechnol*. 2007; 25:327. [PubMed: 17334358]
99. Valadon P, Darsow B, Buss TN, Czarny M, Griffin NM, Nguyen HN, Oh P, Borgstrom P, Chrastina A, Schnitzer JE. *J Biol Chem*. 2010; 285:713. [PubMed: 19850928]
100. Garanger E, Boturyn D, Dumy P. *Anticancer Agents Med Chem*. 2007; 7:552. [PubMed: 17896915]
101. Ferro-Flores G, Ramirez Fde M, Melendez-Alafort L, Santos-Cuevas CL. *Mini Rev Med Chem*. 2010; 10:87. [PubMed: 20380643]
102. Jayasena S. *Clinical chemistry*. 1999; 45:1628. [PubMed: 10471678]
103. Golden M, Collins B, Willis M, Koch T. *Journal of biotechnology*. 2000; 81:167. [PubMed: 10989176]
104. Bunka D, Stockley P. *Nature Reviews Microbiology*. 2006; 4:588.
105. Farokhzad OC, Jon S, Khademhosseini A, Tran TN, Lavan DA, Langer R. *Cancer Res*. 2004; 64:7668. [PubMed: 15520166]
106. Farokhzad OC, Cheng J, Teply BA, Sherifi I, Jon S, Kantoff PW, Richie JP, Langer R. *Proc Natl Acad Sci U S A*. 2006; 103:6315. [PubMed: 16606824]
107. Farokhzad OC, Karp JM, Langer R. *Expert Opin Drug Deliv*. 2006; 3:311. [PubMed: 16640493]
108. Dhar S, Gu FX, Langer R, Farokhzad OC, Lippard SJ. *Proc Natl Acad Sci U S A*. 2008; 105:17356. [PubMed: 18978032]
109. Gu F, Zhang L, Teply BA, Mann N, Wang A, Radovic-Moreno AF, Langer R, Farokhzad OC. *Proc Natl Acad Sci U S A*. 2008; 105:2586. [PubMed: 18272481]
110. Kolishetti N, Dhar S, Valencia PM, Lin LQ, Karnik R, Lippard SJ, Langer R, Farokhzad OC. *Proc Natl Acad Sci U S A*. 2010; 107:17939. [PubMed: 20921363]
111. Li SD, Huang L. *Mol Pharm*. 2006; 3:579. [PubMed: 17009857]
112. Chono S, Li SD, Conwell CC, Huang L. *J Control Release*. 2008; 131:64. [PubMed: 18674578]
113. Li SD, Chen YC, Hackett MJ, Huang L. *Mol Ther*. 2008; 16:163. [PubMed: 17923843]
114. Li SD, Chono S, Huang L. *Mol Ther*. 2008; 16:942. [PubMed: 18388916]
115. Li SD, Chono S, Huang L. *J Control Release*. 2008; 126:77. [PubMed: 18083264]
116. Chen Y, Sen J, Bathula SR, Yang Q, Fittipaldi R, Huang L. *Mol Pharm*. 2009; 6:696. [PubMed: 19267451]
117. Chen Y, Bathula SR, Yang Q, Huang L. *J Invest Dermatol*. 2010; 130:2790. [PubMed: 20686495]
118. Nakagawa O, Ming X, Huang L, Juliano RL. *J Am Chem Soc*. 2010; 132:8848. [PubMed: 20550198]
119. Reddy BS, Banerjee R. *Angew Chem Int Ed Engl*. 2005; 44:6723. [PubMed: 16187396]
120. Kiessling LL, Gestwicki JE, Strong LE. *Angewandte Chemie International Edition*. 2006; 45:2348.
121. Zhao Y, Tian Y, Cui Y, Liu W, Ma W, Jiang X. *J Am Chem Soc*. 2010; 132:12349. [PubMed: 20707350]
122. Bowman M, Ballard T, Ackerson C, Feldheim D, Margolis D, Melander C. *Journal of the American Chemical Society*. 2008; 130:6896. [PubMed: 18473457]

123. Wu K, Liu J, Johnson RN, Yang J, Kopecek J. *Angew Chem Int Ed Engl.* 2010; 49:1451. [PubMed: 20101660]
124. Muro S, Garnacho C, Champion JA, Leferovich J, Gajewski C, Schuchman EH, Mitragotri S, Muzykantov VR. *Molecular Therapy.* 2008; 16:1450. [PubMed: 18560419]
125. Bhattacharyya S, Bhattacharya R, Curley S, McNiven MA, Mukherjee P. *Proc Natl Acad Sci U S A.* 2010; 107:14541. [PubMed: 20679244]
126. Venturoli D, Rippe B. *Am J Physiol Renal Physiol.* 2005; 288:F605. [PubMed: 15753324]
127. Yuan F, Dellian M, Fukumura D, Leunig M, Berk DA, Torchilin VP, Jain RK. *Cancer Res.* 1995; 55:3752. [PubMed: 7641188]
128. Li SD, Huang L. *J Control Release.* 2010; 145:178. [PubMed: 20338200]
129. Young KD. *Curr Opin Microbiol.* 2007; 10:596. [PubMed: 17981076]
130. Geng Y, Dalhaimer P, Cai S, Tsai R, Tewari M, Minko T, Discher DE. *Nat Nanotechnol.* 2007; 2:249. [PubMed: 18654271]
131. Guck J, Schinkinger S, Lincoln B, Wottawah F, Ebert S, Romeyke M, Lenz D, Erickson HM, Ananthakrishnan R, Mitchell D, Kas J, Ulvick S, Bilby C. *Biophys J.* 2005; 88:3689. [PubMed: 15722433]
132. Lee GY, Lim CT. *Trends Biotechnol.* 2007; 25:111. [PubMed: 17257698]
133. Merkel TJ, Jones SW, Herlihy KP, Kersey FR, Shields AR, Napier M, Luft JC, Wu H, Zamboni WC, Wang AZ, Bear JE, DeSimone JM. *Proc Natl Acad Sci U S A.* 2010
134. Alexis F, Pridgen E, Molnar LK, Farokhzad OC. *Mol Pharm.* 2008; 5:505. [PubMed: 18672949]
135. Yamamoto Y, Nagasaki Y, Kato Y, Sugiyama Y, Kataoka K. *J Control Release.* 2001; 77:27. [PubMed: 11689257]
136. He C, Hu Y, Yin L, Tang C, Yin C. *Biomaterials.* 2010; 31:3657. [PubMed: 20138662]
137. Fang C, Shi B, Pei YY, Hong MH, Wu J, Chen HZ. *Eur J Pharm Sci.* 2006; 27:27. [PubMed: 16150582]
138. Weissleder R, Kelly K, Sun EY, Shtatland T, Josephson L. *Nature Biotechnology.* 2005; 23:1418.

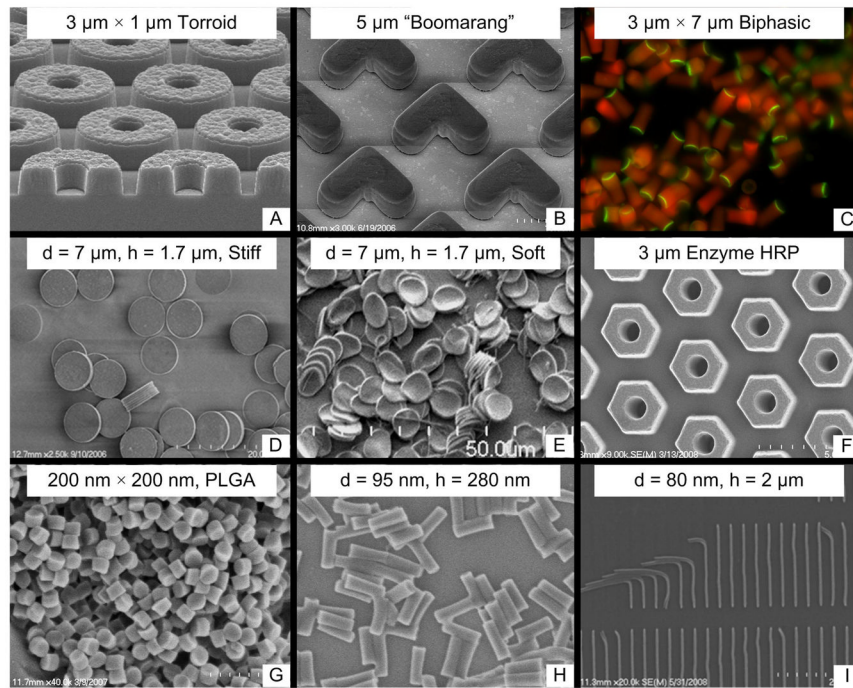


Figure 1.

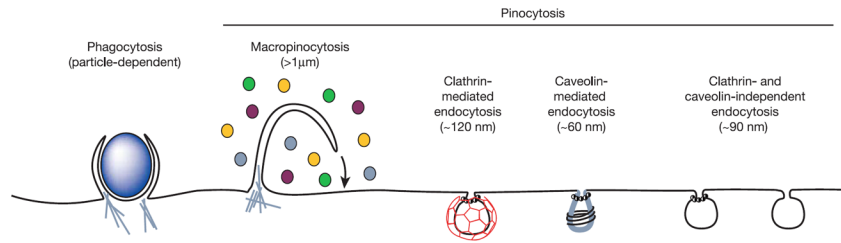


Figure 2.

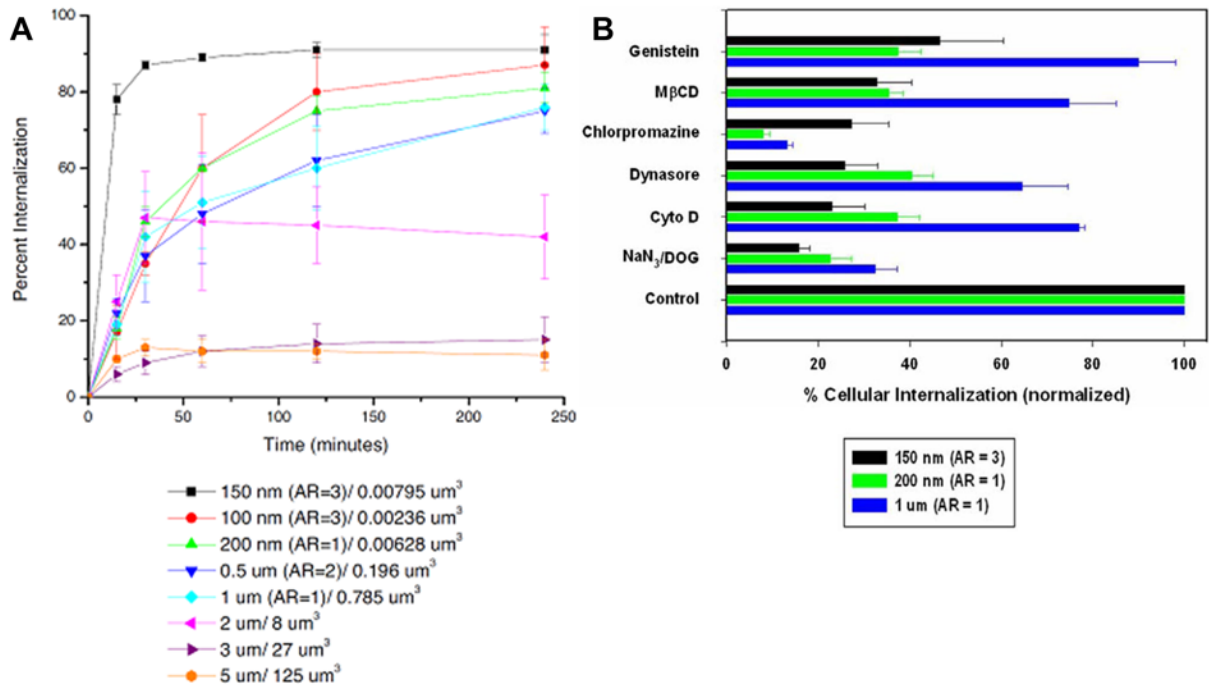
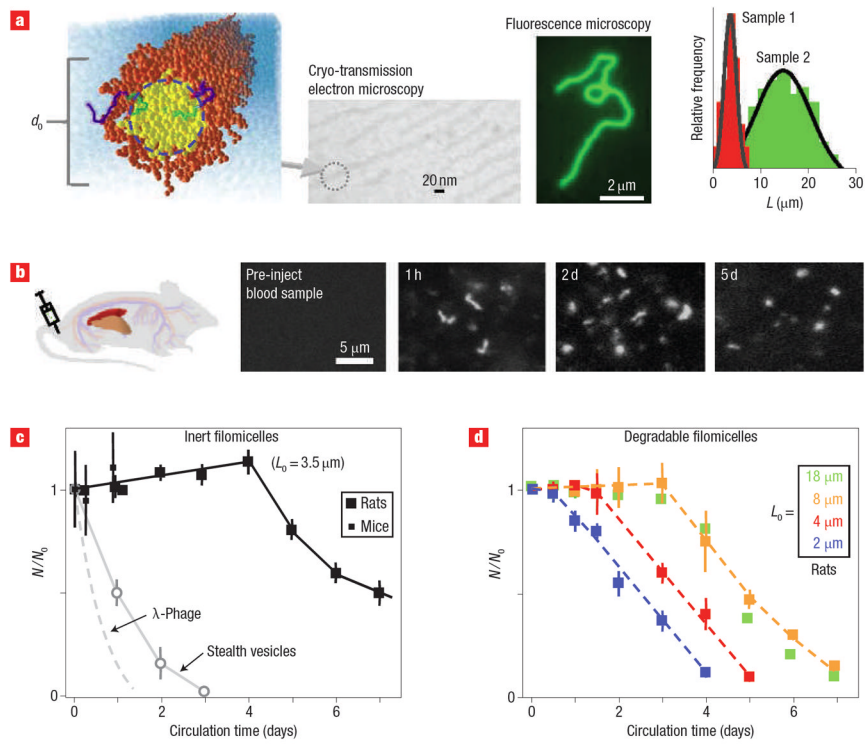


Figure 3.





**Figure 4.**

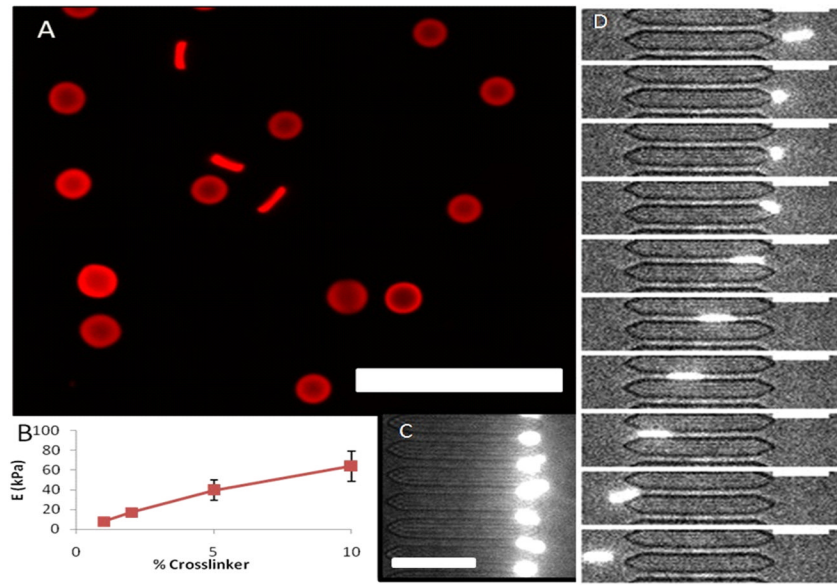
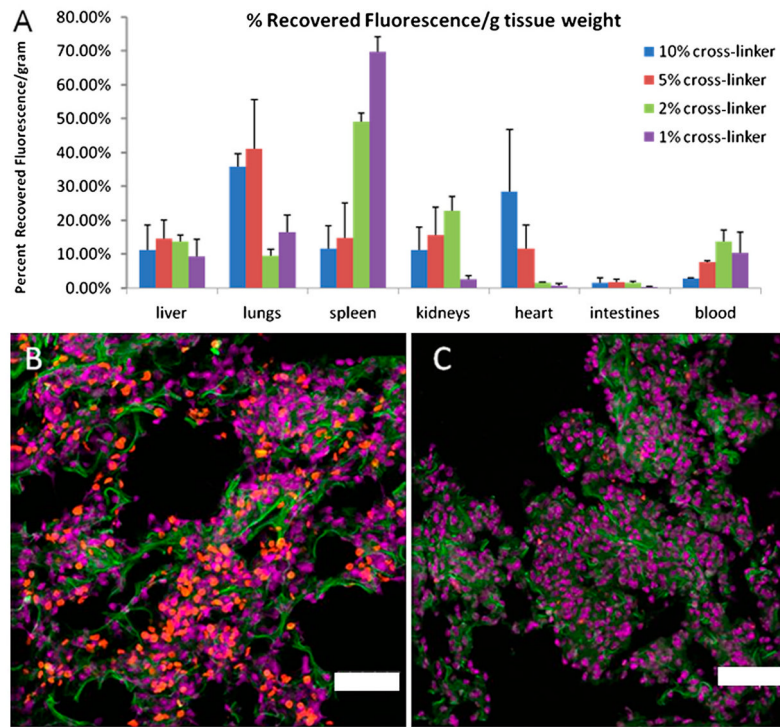


Figure 5.



**Figure 6.**